

Chapter 4 (part 2)

Marcelo Arcanjo

Dena Desarrollos, S.L. (INGESCO)

Universitat Politècnica de Catalunya (UPC)

- 4.4 Stepped Leader
 - 4.4.7 Streamer zone
 - 4.4.8 Step-formation mechanism
- 4.5 Attachment process
 - 4.5.1 Time-resolved optical images
 - 4.5.2 Still photographs
- 4.6 Return Stroke
 - 4.6.1 Parameters derived from channel base current measurements
 - 4.6.2 Luminosity variation along the channel and propagation speed
 - 4.6.3 Measured electric and magnetic fields
 - 4.6.4 Calculation of electric and magnetic fields
 - 4.6.5 Properties of the return-stroke channel

- 4.4 Stepped Leader
 - 4.4.7 Streamer zone
 - 4.4.8 Step-formation mechanism
- 4.5 Attachment process
 - 4.5.1 Time-resolved optical images
 - 4.5.2 Still photographs
- 4.6 Return Stroke
 - 4.6.1 Parameters derived from channel base current measurements
 - 4.6.2 Luminosity variation along the channel and propagation speed
 - 4.6.3 Measured electric and magnetic fields
 - 4.6.4 Calculation of electric and magnetic fields
 - 4.6.5 Properties of the return-stroke channel

4.4 Stepped Leader

4.4.7 and 4.4.8 – Streamer Zone and stepping formation mechanism

- Rakov and Uman show several analysis using streak photography, provoking a time-varying deflection of the light across the width of the detector.

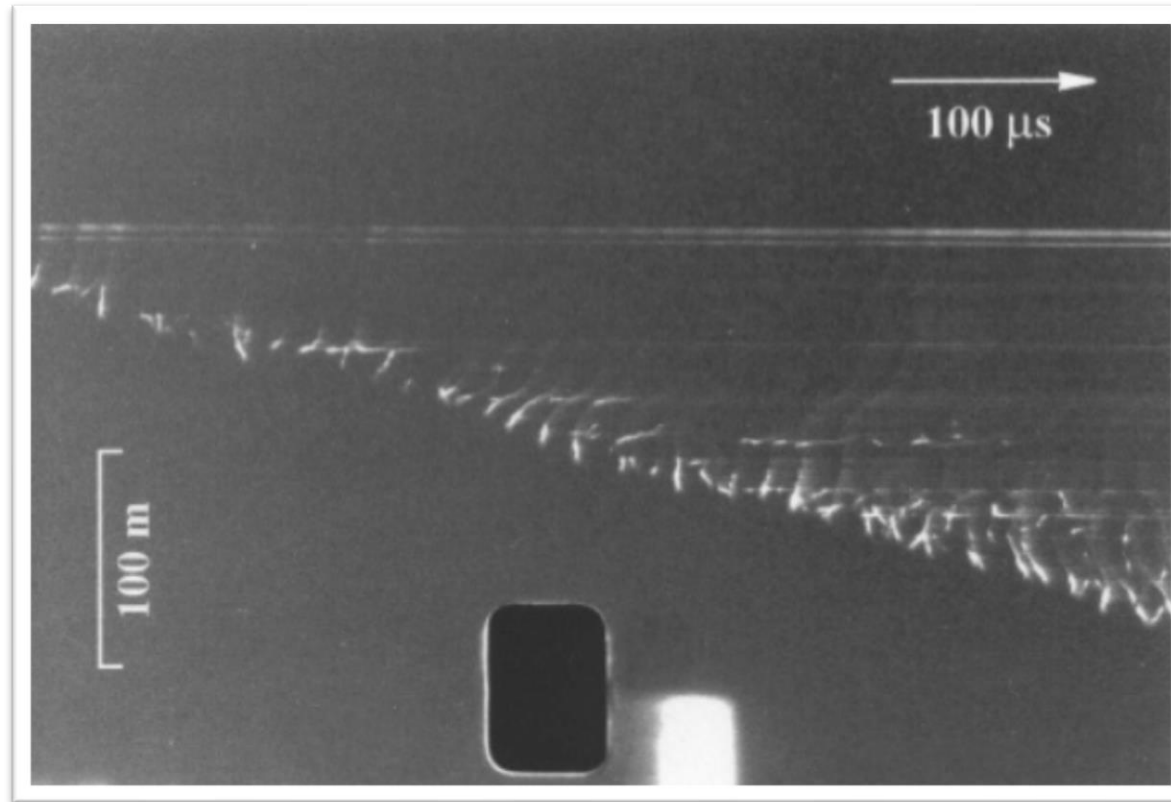


Fig. 7.6. Near-ultraviolet streak-camera record of the downward negative leader in KSC altitude-triggered lightning flash 9119. Time advances from left to right. Adapted from Idone (1992).

4.4 Stepped Leader

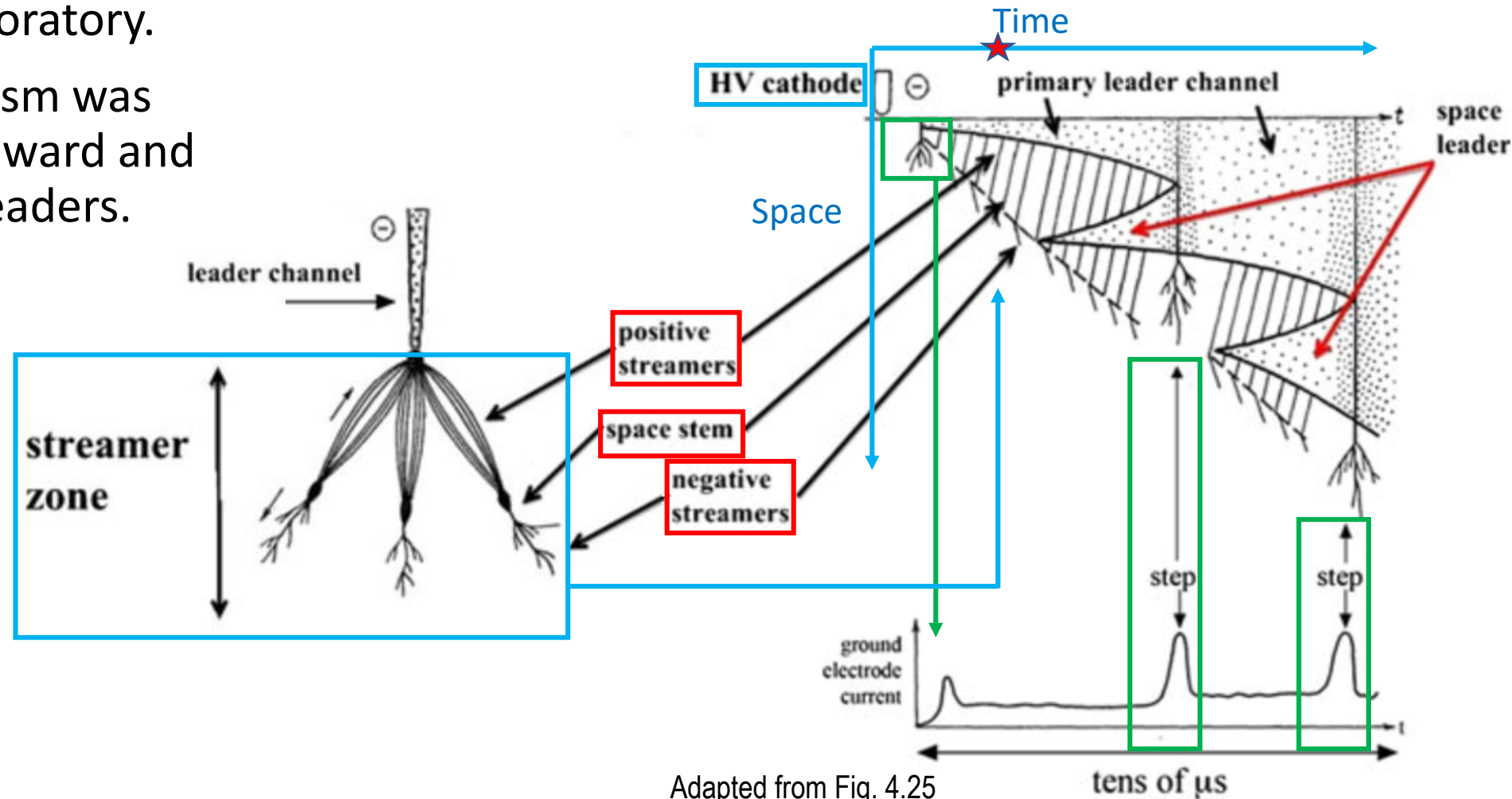
4.4.7 and 4.4.8 – Streamer Zone and stepping formation mechanism

- Several authors, using streak photography, reported cases of a brushed-like corona occurring ahead of the upward-moving negative leader tip in upward positive lightning.
- However, for downward negative leaders, the observation was not reported, or if so, it was reported as a faint luminosity extending below the bottom of a bright step.

4.4 Stepped Leader

4.4.7 and 4.4.8 – Streamer Zone and stepping formation mechanism

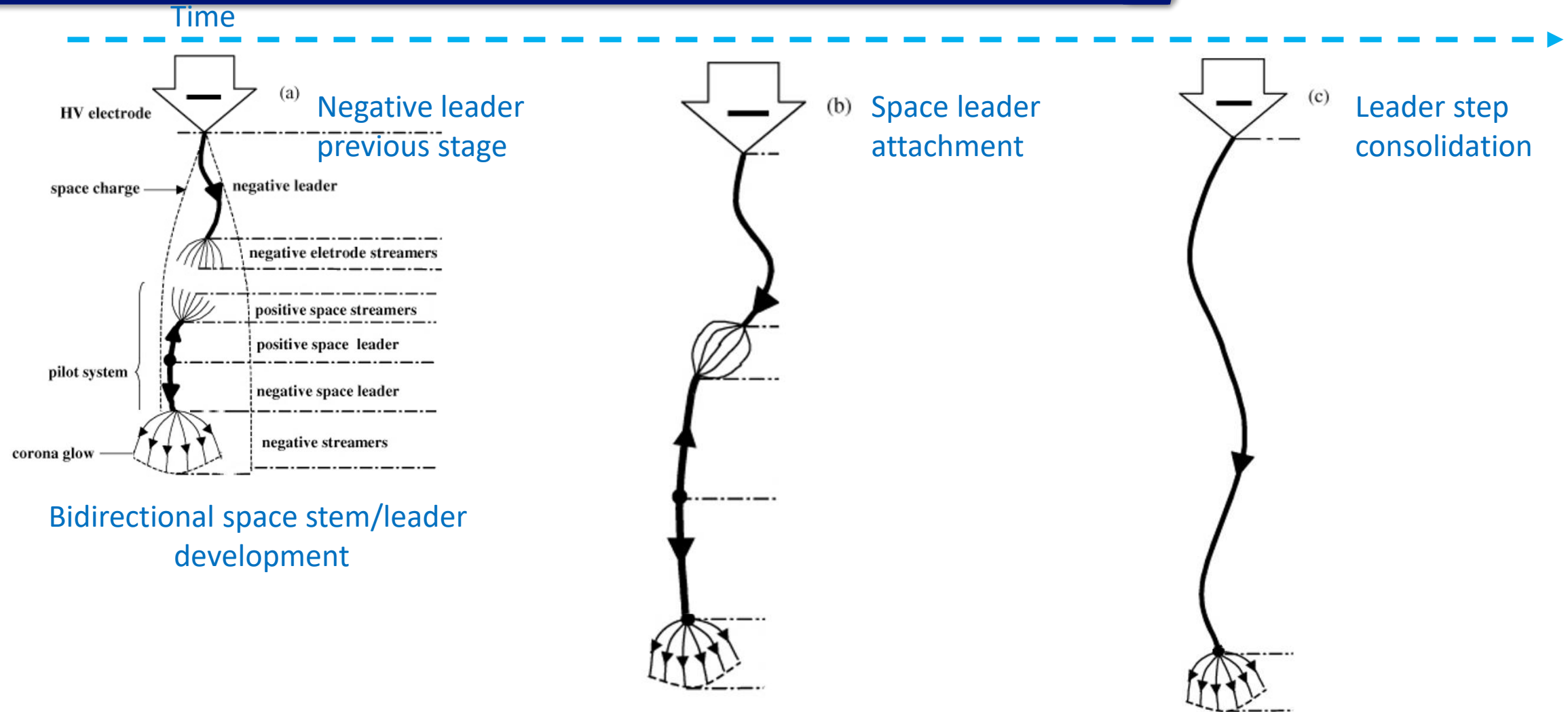
- The stepping formation for lightning negative leaders is similar to long spark experiments in laboratory.
- The same mechanism was observed for downward and upward negative leaders.



Adapted from Fig. 4.25

4.4 Stepped Leader

4.4.7 and 4.4.8 – Streamer Zone and stepping formation mechanism

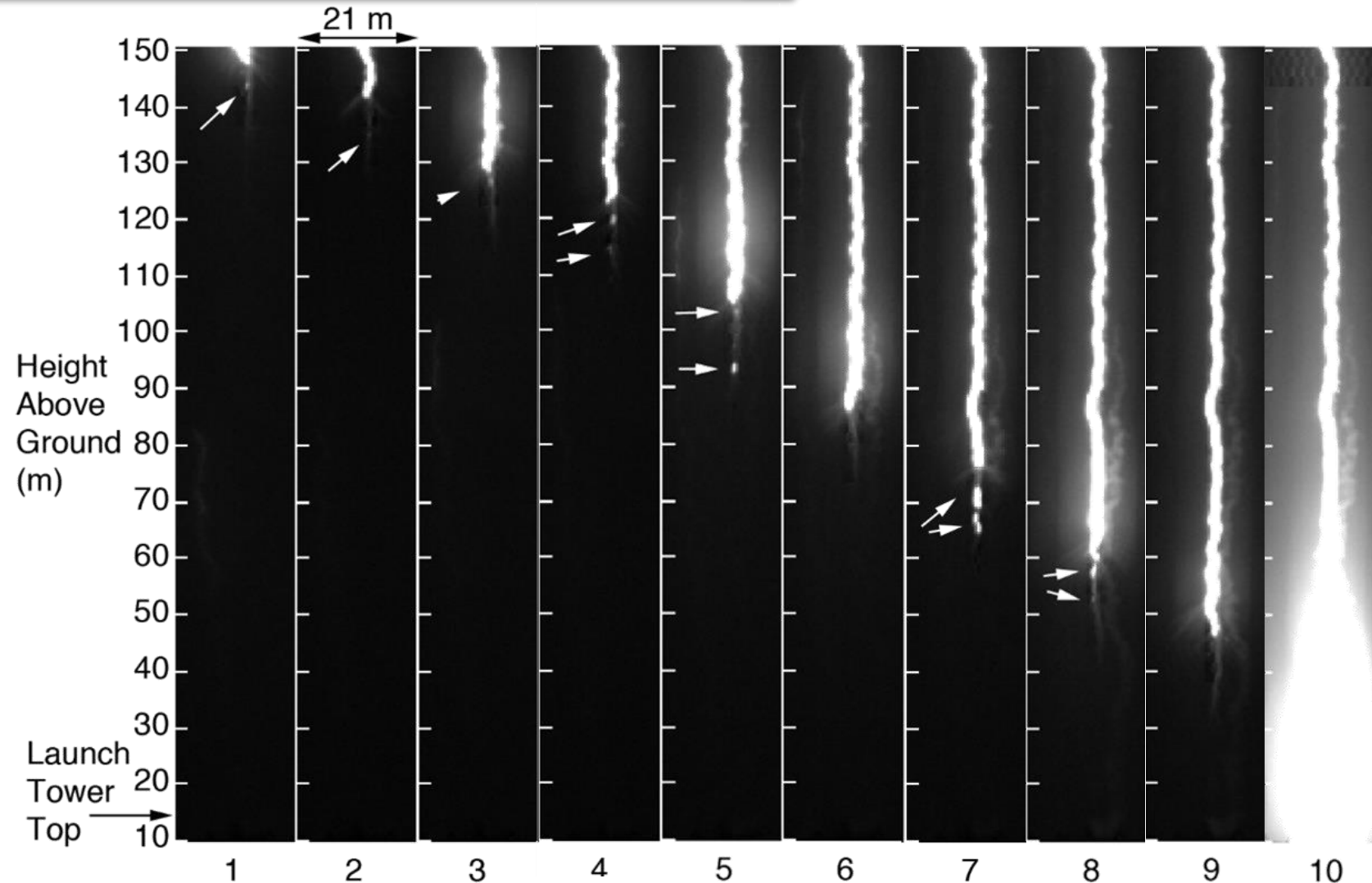


Supplementary Image¹: Rakotonandrasana *et al* 2008

4.4 Stepped Leader

4.4.7 and 4.4.8 – Streamer Zone and stepping formation mechanism

- Recent observations of space leaders in negative cloud-to-ground lightning.
- Brighter segments of light formed just below a faint luminous connection with the downward leader.



Supplementary Image²: Biagi *et al* 2010 .

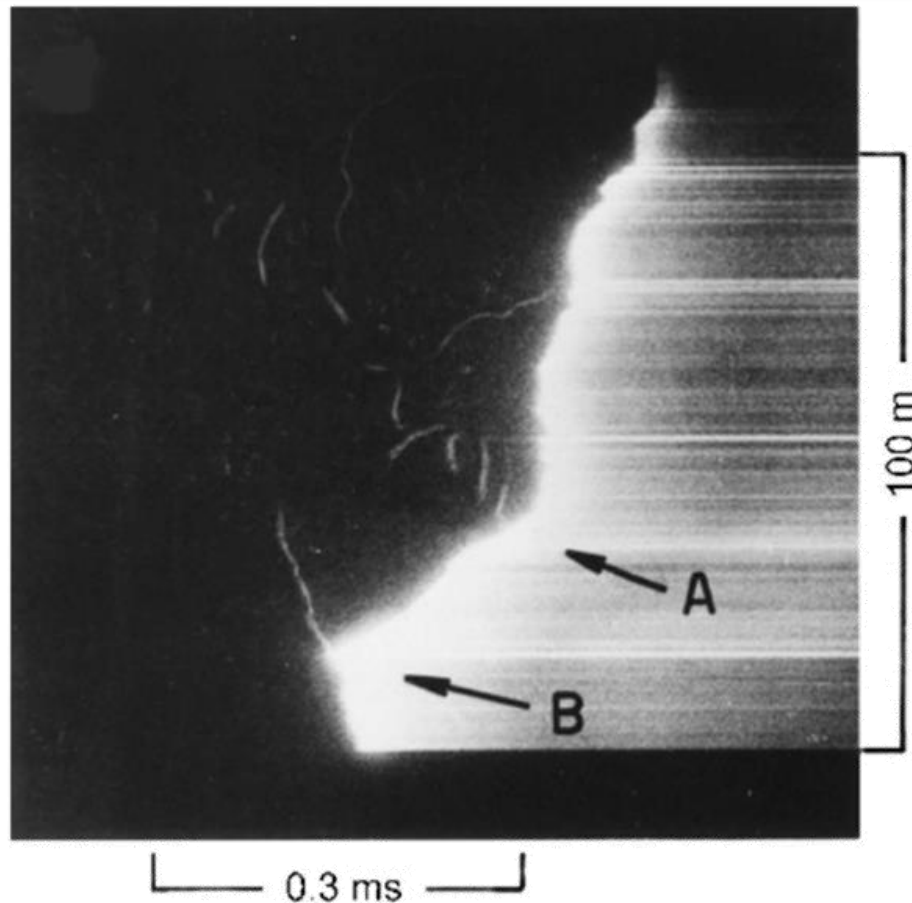
- 4.4 Stepped Leader
 - 4.4.7 Streamer zone
 - 4.4.8 Step-formation mechanism
- 4.5 Attachment process
 - 4.5.1 Time-resolved optical images
 - 4.5.2 Still photographs
- 4.6 Return Stroke
 - 4.6.1 Parameters derived from channel base current measurements
 - 4.6.2 Luminosity variation along the channel and propagation speed
 - 4.6.3 Measured electric and magnetic fields
 - 4.6.4 Calculation of electric and magnetic fields
 - 4.6.5 Properties of the return-stroke channel

- Is one of the least understood processes of the cloud-to-ground lightning discharge;
- General overview:
 - In response to an approaching downward-moving leader, an upward-moving leader is initiated at the ground (or at a tip of an object connected to the ground). It is possible that two or more upward leaders are launched toward the descending leader.
 - ***Upward connecting leader***: An upward leader that makes contact with a branch of a downward leader;
 - ***Unconnected upward leader***: An upward leader that fails to make such a contact.

- The process by which the extending plasma channels of the upward and downward leaders make contact is called the **break-through phase** or **final jump**.
 - The relatively low-conductivity streamer zones ahead of the two propagating leader tips meet to form a **common streamer zone**.
 - The extension of the two relatively high-conductivity plasma channels toward each other takes place inside the common streamer zone.
- The break-through phase can be viewed as a switch-closing operation that serves to launch two return-stroke waves from the point of junction between the two plasma channels.
 - One wave moves downward, toward the ground, and the other upward, towards the cloud.
- The attachment process occurs in both first and subsequent lightning strokes.

4.5 Attachment Process

4.5.1 – Time-resolved optical images



(a)



(b)

Fig. 4.26. (a) Streak-camera photograph of a lightning discharge to a tower on Monte San Salvatore, Switzerland, showing evidence of an upward connecting leader. (b) Still photograph of the same flash and another flash that attached to the tower below its top. Adapted from Berger and Vogelsanger (1966).

4.5 Attachment Process

4.5.2 – Still photographs



Fig. 4.28. A photograph of a lightning strike to a chimney pot showing a split in the channel, interpreted as evidence of an upward connecting leader. Adapted from Golde (1967).



Fig. 4.29. Photograph of a lightning strike to a European ash in Lugano, Switzerland showing both downward and upward branching. From Orville (1968e).



Fig. 4.32. Photograph of a lightning strike to a TV tower guy wire showing an abrupt change in channel shape near the attachment point. Taken from Krider and Alejandro (1983).

4.5 Attachment Process

4.5.2 – Still photographs

- Fig. 4.30 exhibits both upward and downward **branches** originating from the main channel and unconnected upward discharges originating from the ground near the strike point.

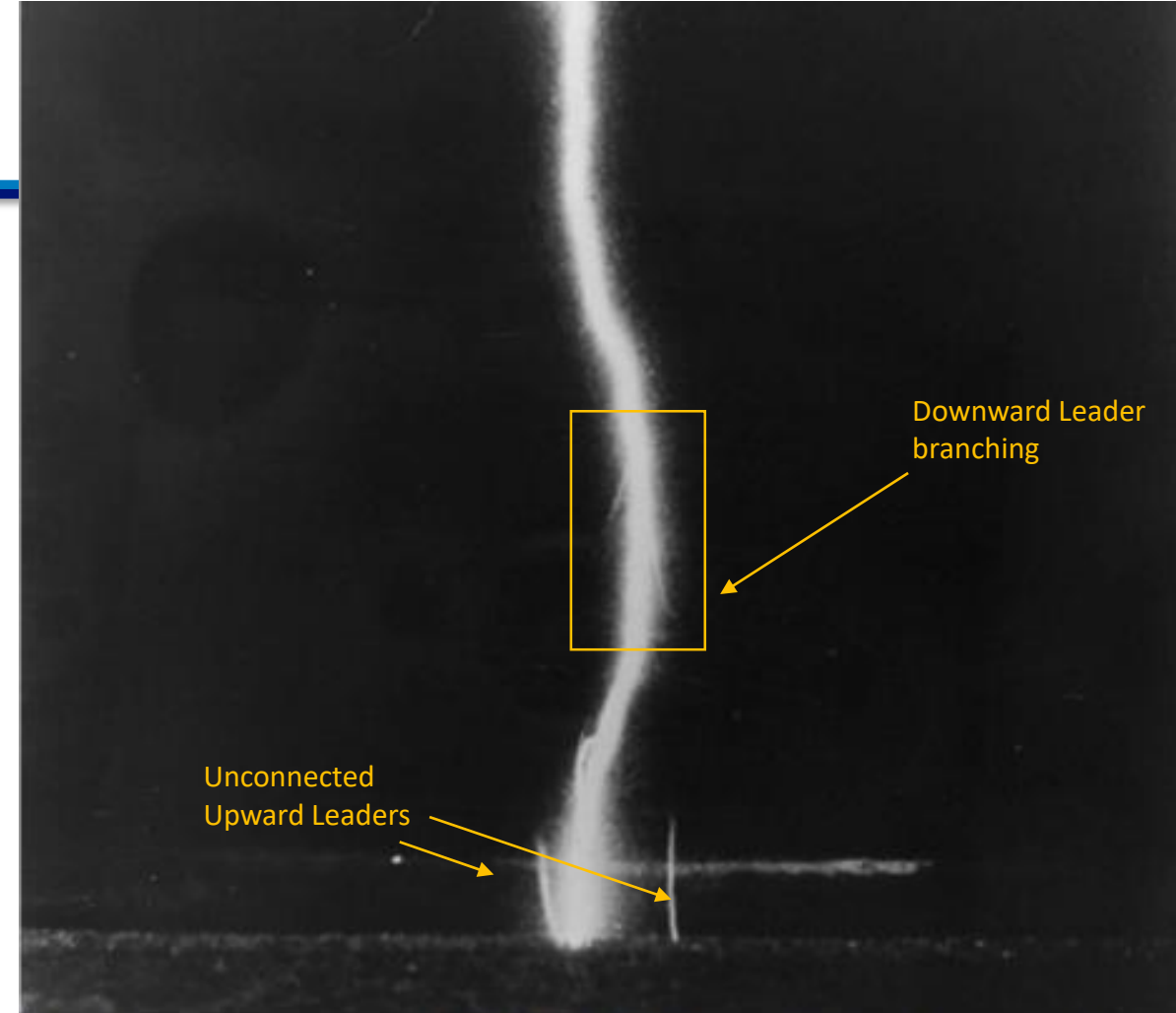
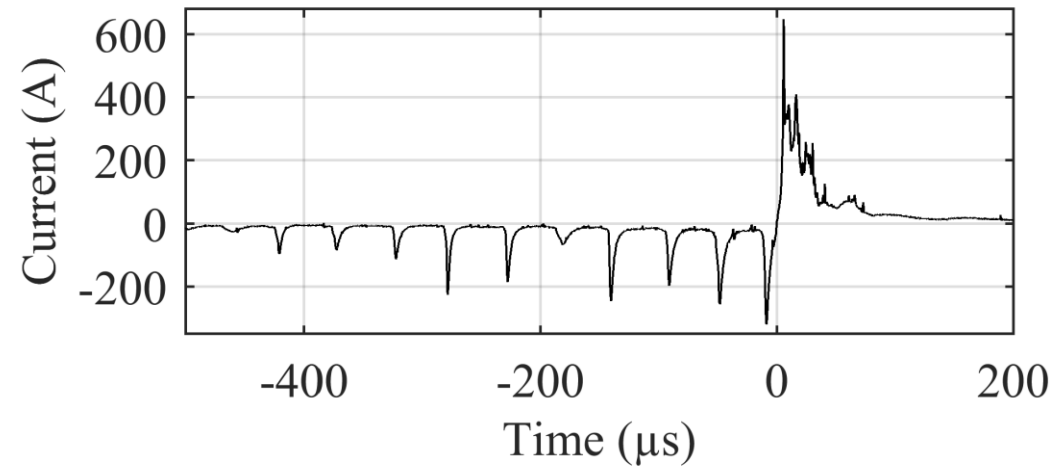


Fig. 4.30. Photograph by Robert Edwards of a lightning strike to the sand at Manasquan Beach, New Jersey taken in July 1934 from a distance of about 30 m. Note both downward and upward branching, and an unconnected discharge from the ground to the right of the main lightning channel.

4.5 Attachment Process

4.5.2 – Still photographs

- Unconnected Upward discharges have been observed in both triggered and natural lightning. From still photographs, upward leaders with a few meters in height were recorder near the termination of lightning discharges.



Supplementary Image³: Arcanjo et al. 2019.

- 4.4 Stepped Leader
 - 4.4.7 Streamer zone
 - 4.4.8 Step-formation mechanism
- 4.5 Attachment process
 - 4.5.1 Time-resolved optical images
 - 4.5.2 Still photographs
- 4.6 Return Stroke
 - 4.6.1 Parameters derived from channel base current measurements
 - 4.6.2 Luminosity variation along the channel and propagation speed
 - 4.6.3 Measured electric and magnetic fields
 - 4.6.4 Calculation of electric and magnetic fields
 - 4.6.5 Properties of the return-stroke channel

4.6 Return Stroke

4.6.1 – Parameters derived from channel base current measurements

- The most complete characterization of the return stroke in the negative downward flash striking short structures (< 100 m) or flat terrain is due to Karl Berger. These measurements were performed using resistive shunts installed at the tops of two 70-m-high towers on the summit of Monte San Salvatore in Lugano, Switzerland.

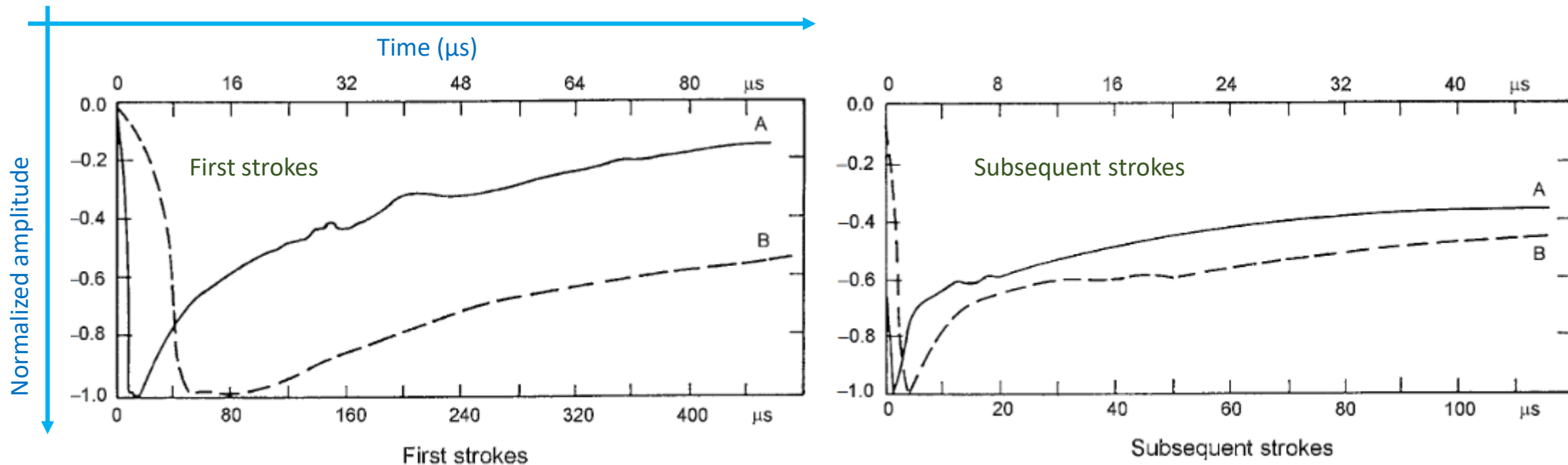


Fig. 4.33. Average negative first- and subsequent-stroke current waveshapes each shown on two time scales, A and B.

4.6 Return Stroke

4.6.1 – Parameters derived from channel base current measurements

Table 4.4. Parameters of downward negative lightning derived from channel-base current measurements. Adapted from Berger et al. (1975)

Parameters	Units	Sample size	Percentage exceeding tabulated value		
			95%	50%	5%
Peak current (minimum 2 kA)	kA				
First strokes		101	14	30	80
Subsequent strokes		135	4.6	12	30
Charge (total charge)	C				
First strokes		93	1.1	5.2	24
Subsequent strokes		122	0.2	1.4	11
Complete flash		94	1.3	7.5	40
Impulse charge (excluding continuing current)	C				
First strokes		90	1.1	4.5	20
Subsequent strokes		117	0.22	0.95	4
Front duration (2 kA to peak)	µs				
First strokes		89	1.8	5.5	18
Subsequent strokes		118	0.22	1.1	4.5
Maximum di/dt	kA µs ⁻¹				
First strokes		92	5.5	12	32
Subsequent strokes		122	12	40	120
Stroke duration (2 kA to half peak value on the tail)	µs				
First strokes		90	30	75	200
Subsequent strokes		115	6.5	32	140
Action integral (∫ I dt)	A² s				
First strokes		91	6.0 × 10³	5.5 × 10⁴	5.5 × 10⁵
Subsequent strokes		88	5.5 × 10²	6.0 × 10³	5.2 × 10⁴
Time interval between strokes	ms	133	7	33	150
Flash duration	ms				
All flashes		94	0.15	13	1100
Excluding single-stroke flashes		39	31	180	900

Table 4.4. Parameters of downward negative lightning derived from channel-base current measurements. Adapted from Berger et al. (1975)

Parameters	Units	Sample size	Percentage exceeding tabulated value		
			95%	50%	5%
Peak current (minimum 2 kA)	kA				
First strokes		101	14	30	80
Subsequent strokes		135	4.6	12	30

4.6 Return Stroke

4.6.1 – Parameters derived from channel base current measurements

- Charge transferred:

$$Q = \int_0^T i(t) dt$$

Table 4.4. Parameters of downward negative lightning derived from channel-base current measurements. Adapted from Berger et al. (1975)

Parameters	Units	Sample size	Percentage exceeding tabulated value		
			95%	50%	5%
Peak current (minimum 2 kA)	kA				
First strokes		101	14	30	80
Subsequent strokes		135	4.6	12	30
Charge (total charge)	C				
First strokes		93	1.1	5.2	24
Subsequent strokes		122	0.2	1.4	11
Complete flash		94	1.3	7.5	40
Impulse charge (excluding continuing current)	C				
First strokes		90	1.1	4.5	20
Subsequent strokes		117	0.22	0.95	4
Front duration (2 kA to peak)	μs				
First strokes		89	1.8	5.5	18
Subsequent strokes		118	0.22	1.1	4.5
Maximum di/dt	kA μs ⁻¹				
First strokes		92	5.5	12	32
Subsequent strokes		122	12	40	120
Stroke duration (2 kA to half peak value on the tail)	μs				
First strokes		90	30	75	200
Subsequent strokes		115	6.5	32	140
Action integral (∫ I dt)	A ² s				
First strokes		91	6.0 × 10 ³	5.5 × 10 ⁴	5.5 × 10 ⁵
Subsequent strokes		88	5.5 × 10 ²	6.0 × 10 ³	5.2 × 10 ⁴
Time interval between strokes	ms	133	7	33	150
Flash duration	ms				
All flashes		94	0.15	13	1100
Excluding single-stroke flashes		39	31	180	900

Table 4.4. Parameters of downward negative lightning derived from channel-base current measurements. Adapted from Berger et al. (1975)

Parameters	Units	Sample size	Percentage exceeding tabulated value		
			95%	50%	5%
Charge (total charge)	C				
First strokes		93	1.1	5.2	24
Subsequent strokes		122	0.2	1.4	11
Complete flash		94	1.3	7.5	40
Impulse charge (excluding continuing current)	C				
First strokes		90	1.1	4.5	20
Subsequent strokes		117	0.22	0.95	4

4.6 Return Stroke

4.6.1 – Parameters derived from channel base current measurements

Table 4.4. Parameters of downward negative lightning derived from channel-base current measurements. Adapted from Berger et al. (1975)

Parameters	Units	Sample size	Percentage exceeding tabulated value		
			95%	50%	5%
Peak current (minimum 2 kA)	kA				
First strokes		101	14	30	80
Subsequent strokes		135	4.6	12	30
Charge (total charge)	C				
First strokes		93	1.1	5.2	24
Subsequent strokes		122	0.2	1.4	11
Complete flash		94	1.3	7.5	40
Impulse charge (excluding continuing current)	C				
First strokes		90	1.1	4.5	20
Subsequent strokes		117	0.22	0.95	4
Front duration (2 kA to peak)	μs				
First strokes		89	1.8	5.5	18
Subsequent strokes		118	0.22	1.1	4.5
Maximum di/dt	kA μs ⁻¹				
First strokes		92	5.5	12	32
Subsequent strokes		122	12	40	120
Stroke duration (2 kA to half peak value on the tail)	μs				
First strokes		90	30	75	200
Subsequent strokes		115	6.5	32	140
Action integral (∫ I dt)	A ² s				
First strokes		91	6.0 × 10 ³	5.5 × 10 ⁴	5.5 × 10 ⁵
Subsequent strokes		88	5.5 × 10 ²	6.0 × 10 ³	5.2 × 10 ⁴
Time interval between strokes	ms	133	7	33	150
Flash duration	ms				
All flashes		94	0.15	13	1100
Excluding single-stroke flashes		39	31	180	900

Table 4.4. Parameters of downward negative lightning derived from channel-base current measurements. Adapted from Berger et al. (1975)

Parameters	Units	Sample size	Percentage exceeding tabulated value		
			95%	50%	5%
Front duration (2 kA to peak)	μs				
First strokes		89	1.8	5.5	18
Subsequent strokes		118	0.22	1.1	4.5

4.6 Return Stroke

4.6.1 – Parameters derived from channel base current measurements

- Current derivative:

$$S = \frac{di(t)}{dt}$$

Table 4.4. Parameters of downward negative lightning derived from channel-base current measurements. Adapted from Berger et al. (1975)

Parameters	Units	Sample size	Percentage exceeding tabulated value		
			95%	50%	5%
Peak current (minimum 2 kA)	kA				
First strokes		101	14	30	80
Subsequent strokes		135	4.6	12	30
Charge (total charge)	C				
First strokes		93	1.1	5.2	24
Subsequent strokes		122	0.2	1.4	11
Complete flash		94	1.3	7.5	40
Impulse charge (excluding continuing current)	C				
First strokes		90	1.1	4.5	20
Subsequent strokes		117	0.22	0.95	4
Front duration (2 kA to peak)	μs				
First strokes		89	1.8	5.5	18
Subsequent strokes		118	0.22	1.1	4.5
Maximum di/dt	kA μs ⁻¹				
First strokes		92	5.5	12	32
Subsequent strokes		122	12	40	120
Stroke duration (2 kA to half peak value on the tail)	μs				
First strokes		90	30	75	200
Subsequent strokes		115	6.5	32	140
Action integral (∫ I dt)	A ² s				
First strokes		91	6.0 × 10 ³	5.5 × 10 ⁴	5.5 × 10 ⁵
Subsequent strokes		88	5.5 × 10 ²	6.0 × 10 ³	5.2 × 10 ⁴
Time interval between strokes	ms	133	7	33	150
Flash duration	ms				
All flashes		94	0.15	13	1100
Excluding single-stroke flashes		39	31	180	900

Table 4.4. Parameters of downward negative lightning derived from channel-base current measurements. Adapted from Berger et al. (1975)

Parameters	Units	Sample size	Percentage exceeding tabulated value		
			95%	50%	5%
Maximum di/dt	kA μs ⁻¹				
First strokes		92	5.5	12	32
Subsequent strokes		122	12	40	120

4.6 Return Stroke

4.6.1 – Parameters derived from channel base current measurements

Table 4.4. Parameters of downward negative lightning derived from channel-base current measurements. Adapted from Berger et al. (1975)

Parameters	Units	Sample size	Percentage exceeding tabulated value		
			95%	50%	5%
Peak current (minimum 2 kA)	kA				
First strokes		101	14	30	80
Subsequent strokes		135	4.6	12	30
Charge (total charge)	C				
First strokes		93	1.1	5.2	24
Subsequent strokes		122	0.2	1.4	11
Complete flash		94	1.3	7.5	40
Impulse charge (excluding continuing current)	C				
First strokes		90	1.1	4.5	20
Subsequent strokes		117	0.22	0.95	4
Front duration (2 kA to peak)	μs				
First strokes		89	1.8	5.5	18
Subsequent strokes		118	0.22	1.1	4.5
Maximum dI/dt	kA μs ⁻¹				
First strokes		92	5.5	12	32
Subsequent strokes		122	12	40	120
Stroke duration (2 kA to half peak value on the tail)	μs				
First strokes		90	30	75	200
Subsequent strokes		115	6.5	32	140
Action integral (∫ I dt)	A ² s				
First strokes		91	6.0 × 10 ³	5.5 × 10 ⁴	5.5 × 10 ⁵
Subsequent strokes		88	5.5 × 10 ²	6.0 × 10 ³	5.2 × 10 ⁴
Time interval between strokes	ms	133	7	33	150
Flash duration	ms				
All flashes		94	0.15	13	1100
Excluding single-stroke flashes		39	31	180	900

Table 4.4. Parameters of downward negative lightning derived from channel-base current measurements. Adapted from Berger et al. (1975)

Parameters	Units	Sample size	Percentage exceeding tabulated value		
			95%	50%	5%
Stroke duration (2 kA to half peak value on the tail)	μs				
First strokes		90	30	75	200
Subsequent strokes		115	6.5	32	140

4.6 Return Stroke

4.6.1 – Parameters derived from channel base current measurements

- Action integral:

$$W = \int_0^T i^2(t) dt$$

Table 4.4. Parameters of downward negative lightning derived from channel-base current measurements. Adapted from Berger et al. (1975)

Parameters	Units	Sample size	Percentage exceeding tabulated value		
			95%	50%	5%
Peak current (minimum 2 kA)	kA				
First strokes		101	14	30	80
Subsequent strokes		135	4.6	12	30
Charge (total charge)	C				
First strokes		93	1.1	5.2	24
Subsequent strokes		122	0.2	1.4	11
Complete flash		94	1.3	7.5	40
Impulse charge (excluding continuing current)	C				
First strokes		90	1.1	4.5	20
Subsequent strokes		117	0.22	0.95	4
Front duration (2 kA to peak)	μs				
First strokes		89	1.8	5.5	18
Subsequent strokes		118	0.22	1.1	4.5
Maximum di/dt	kA μs ⁻¹				
First strokes		92	5.5	12	32
Subsequent strokes		122	12	40	120
Stroke duration (2 kA to half peak value on the tail)	μs				
First strokes		90	30	75	200
Subsequent strokes		115	6.5	32	140
Action integral ($\int I^2 dt$)	A ² s				
First strokes		91	6.0×10^3	5.5×10^4	5.5×10^5
Subsequent strokes		88	5.5×10^2	6.0×10^3	5.2×10^4
Time interval between strokes	ms	133	7	33	150
Flash duration	ms				
All flashes		94	0.15	13	1100
Excluding single-stroke flashes		39	31	180	900

Table 4.4. Parameters of downward negative lightning derived from channel-base current measurements. Adapted from Berger et al. (1975)

Parameters	Units	Sample size	Percentage exceeding tabulated value		
			95%	50%	5%
Action integral ($\int I^2 dt$)	A ² s				
First strokes		91	6.0×10^3	5.5×10^4	5.5×10^5
Subsequent strokes		88	5.5×10^2	6.0×10^3	5.2×10^4

4.6 Return Stroke

4.6.1 – Parameters derived from channel base current measurements

Table 4.4. Parameters of downward negative lightning derived from channel-base current measurements. Adapted from Berger et al. (1975)

Parameters	Units	Sample size	Percentage exceeding tabulated value		
			95%	50%	5%
Peak current (minimum 2 kA)	kA				
First strokes		101	14	30	80
Subsequent strokes		135	4.6	12	30
Charge (total charge)	C				
First strokes		93	1.1	5.2	24
Subsequent strokes		122	0.2	1.4	11
Complete flash		94	1.3	7.5	40
Impulse charge (excluding continuing current)	C				
First strokes		90	1.1	4.5	20
Subsequent strokes		117	0.22	0.95	4
Front duration (2 kA to peak)	μs				
First strokes		89	1.8	5.5	18
Subsequent strokes		118	0.22	1.1	4.5
Maximum di/dt	kA μs ⁻¹				
First strokes		92	5.5	12	32
Subsequent strokes		122	12	40	120
Stroke duration (2 kA to half peak value on the tail)	μs				
First strokes		90	30	75	200
Subsequent strokes		115	6.5	32	140
Action integral ($\int I dt$)	A ² s				
First strokes		91	6.0×10^3	5.5×10^4	5.5×10^5
Subsequent strokes		88	5.5×10^2	6.0×10^3	5.2×10^4
Time interval between strokes	ms	133	7	33	150
Flash duration	ms				
All flashes		94	0.15	13	1100
Excluding single-stroke flashes		39	31	180	900

Table 4.4. Parameters of downward negative lightning derived from channel-base current measurements. Adapted from Berger et al. (1975)

Parameters	Units	Sample size	Percentage exceeding tabulated value		
			95%	50%	5%
Time interval between strokes	ms	133	7	33	150
Flash duration	ms				
All flashes		94	0.15	13	1100
Excluding single-stroke flashes		39	31	180	900

4.6 Return Stroke

4.6.2 – Luminosity variation along the channel and propagation speed

- The variation in return-stroke luminosity along the channel is thought to reflect the variation in current.
- Figure 4.36 illustrates the time development of the luminosity in the lower portion of a typical first stroke, determined (using streak photography) in South Africa. Upward two-dimensional speeds:
 - 1.6×10^8 m/s from the ground to point A;
 - 2.1×10^8 m/s from A to B;
 - 9.7×10^7 m/s from B to C;
 - 5.5×10^7 m/s from C to D (Schonland 1956).
- When a return stroke reaches a branch, there is usually a brightening of the channel below that point. It is believed that branch components are due to a rapid discharge of a branch, previously charged by the stepped leader.

1×10^8 m/s

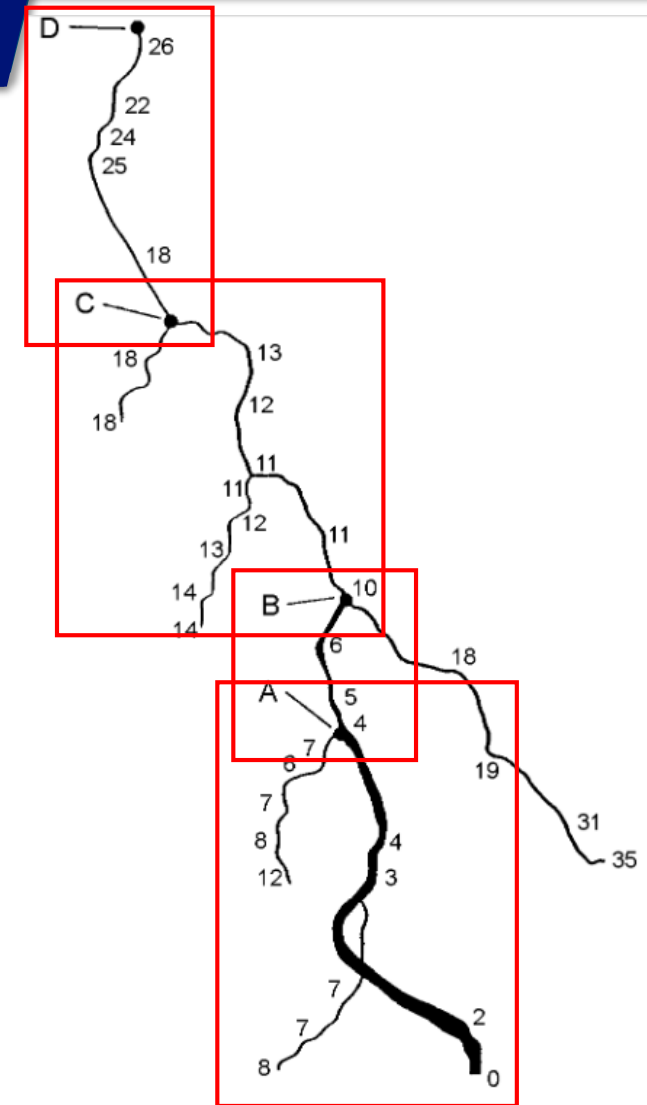


Fig. 4.36. The luminous development of a first return stroke. The numbers indicate the time of arrival in microseconds of the upward-propagating return-stroke front at various points on both the main channel and branches. Adapted from Schonland (1956).

4.6 Return Stroke

4.6.3 – Measured electric and magnetic fields

- Vertical electric and horizontal magnetic field waveforms are shown for distances ranging from 1 to 200 km. As the distance increases, electric and magnetic intensities also decrease in amplitude.
- After the first few tens of microseconds, by the electrostatic component of the total electric field. The **close** magnetic fields at similar times are dominated by the magnetostatic component of the total magnetic field, the component that produces the magnetic field humps.
- The **distant** electric and magnetic fields have essentially identical waveshapes and are usually bipolar. At a distance of 50 km and beyond, both electric and magnetic field wave shapes are dominated by their respective radiation components.

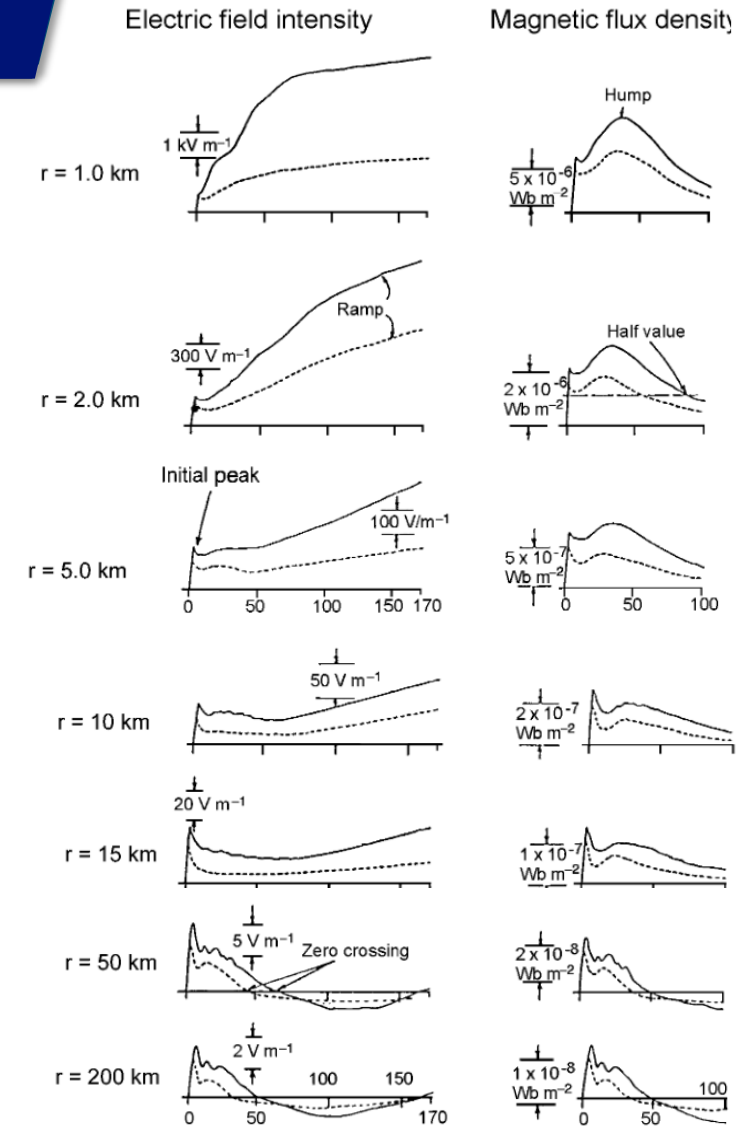


Fig. 4.38. Typical vertical electric field intensity (left column) and azimuthal magnetic flux density (right column) waveforms for first (solid line) and subsequent (broken line) return strokes at distances of 1, 2, 5, 10, 15, 50, and 200 km. The scales are in μs .

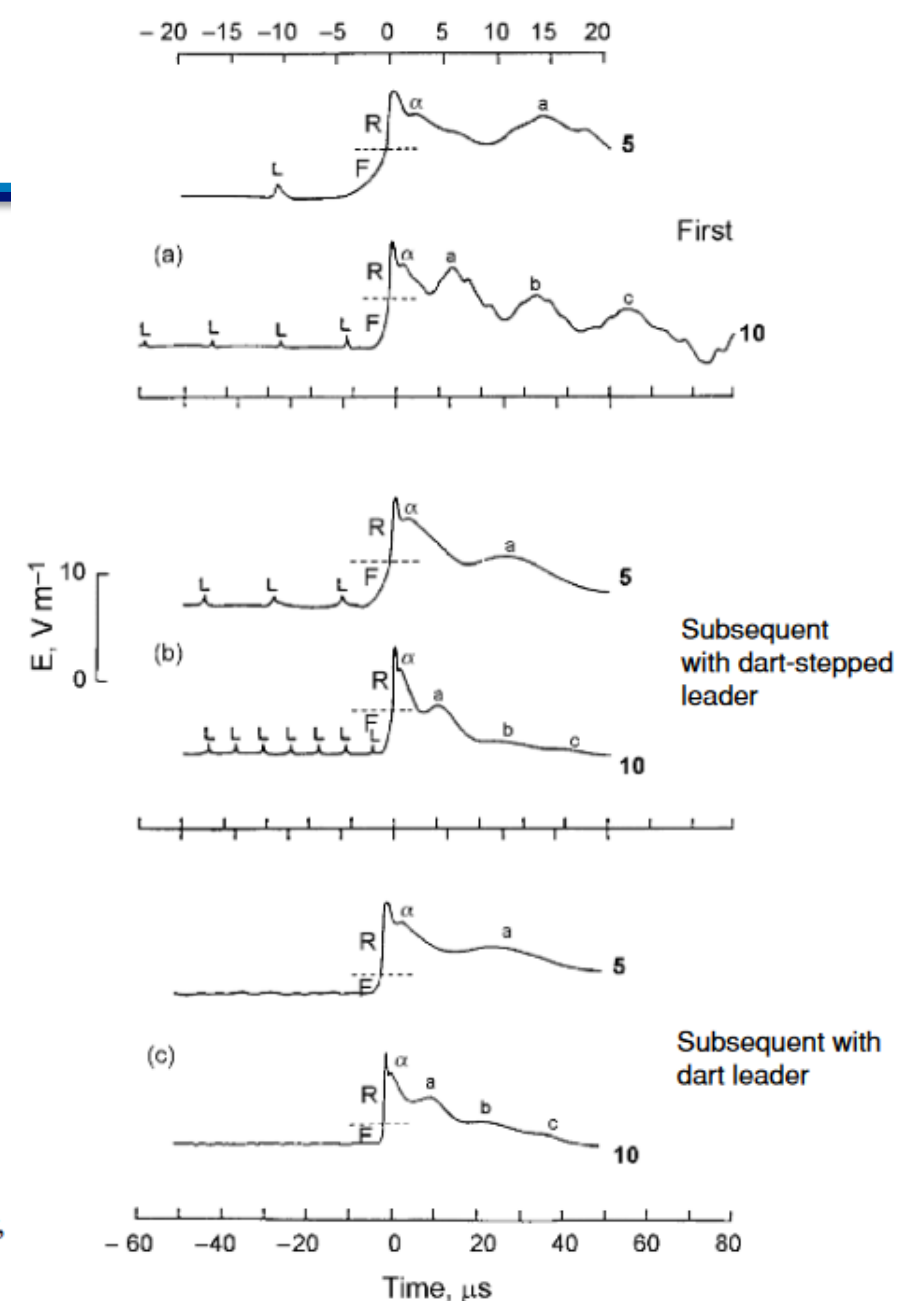
4.6 Return Stroke

4.6.3 – Measured electric and magnetic fields

- As illustrated in Fig. 4.40, first-return-stroke field waveforms have a “slow front” (below the broken line in Fig. 4.40 and labeled F) that rises in a few microseconds to an appreciable fraction of the field peak.
- The slow front is followed by a “fast transition” (labeled R) to peak with a 10–90 percent risetime of about $0.1\mu\text{s}$ when the field propagation path is over saltwater.
- Leader pulses are identified by L, and are observed for the first strokes, dart stepped leaders but not dart leaders.

(scale of upper figures ranges from -20 to 20 μs and the bottom pictures from -60 to 80 μs)

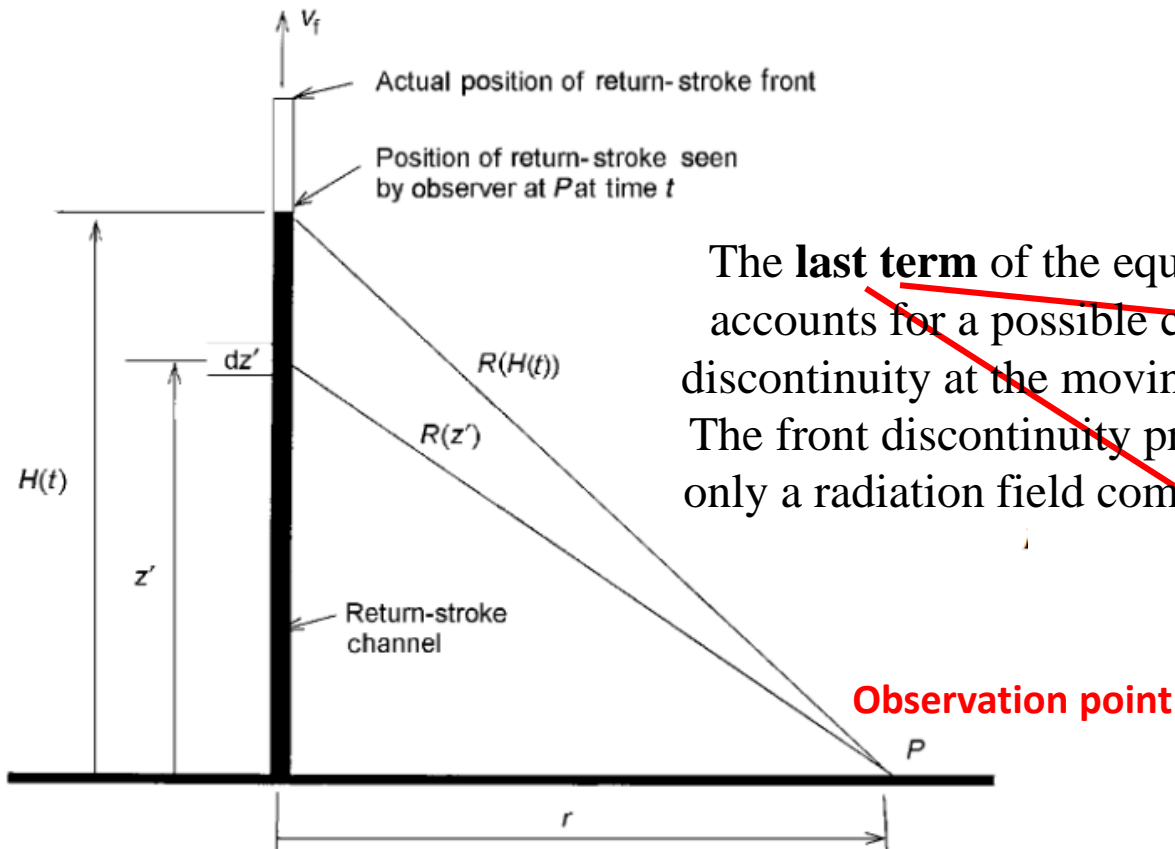
Fig. 4.40. Electric field waveforms of (a) a first return stroke, (b) a subsequent return stroke initiated by a dart-stepped leader, and (c) a subsequent return stroke initiated by a dart leader.



4.6 Return Stroke

4.6.4 – Calculation of electric and magnetic fields

- The most general equations for computing the vertical electric field E_z and azimuthal magnetic field B_ϕ due to an upward-moving return stroke for the case of a field point. P on perfectly conducting ground are:



The **last term** of the equations accounts for a possible current discontinuity at the moving front. The front discontinuity produces only a radiation field component.

$$E_z(r, t) = \frac{1}{2\pi\epsilon_0} \int_0^{H(t)} \left[\frac{2z'^2 - r^2}{R^5(z')} \int_{\frac{z'}{v_f} + \frac{R(z')}{c}}^t I\left(z', \tau - \frac{R(z')}{c}\right) d\tau \right. \\ \left. + \frac{2z'^2 - r^2}{cR^4(z')} I\left(z', t - \frac{R(z')}{c}\right) - \frac{r^2}{c^2 R^3(z')} \frac{\partial I(z', t - R(z')/c)}{\partial t} \right] dz' \\ - \frac{1}{2\pi\epsilon_0} \frac{r^2}{c^2 R^3(H(t))} I\left(H(t), \frac{H(t)}{v_f}\right) \frac{dH(t)}{dt} \quad (4.10)$$

Electrostatic
Induction
Radiation

$$B_\phi(r, t) = \frac{\mu_0}{2\pi} \int_0^{H(t)} \left[\frac{r}{R^3(z')} I\left(z', t - \frac{R(z')}{c}\right) + \frac{r}{cR^2(z')} \frac{\partial I(z', t - R(z')/c)}{\partial t} \right] dz' \\ + \frac{\mu_0}{2\pi} \frac{r}{cR^2(H(t))} I\left(H(t), \frac{H(t)}{v_f}\right) \frac{dH(t)}{dt} \quad (4.11)$$

Magnetostatic
Radiation

4.6 Return Stroke

4.6.4 – Calculation of electric and magnetic fields

- Channel tortuosity and branches
 - In most computations of the fields due to the return stroke, the return-stroke channel is assumed to be straight, while in fact it is known to be tortuous (ranging from 1 m to over 1 km).
 - In general, the effect of tortuosity is to increase the higher-frequency content of the radiation field waveform.
 - Measured first-stroke electric and magnetic fields exhibit a more pronounced fine structure than subsequent strokes, due to the presence of branches in the first strokes.
- Propagation effects
 - At an observation point above a perfectly conducting ground, there are a vertical and horizontal electric field. The horizontal electric field at and below the ground surface is associated with a radial current flow and resultant ohmic losses in the earth.
 - Propagation effects include attenuation of the higher-frequency components in the vertical electric field and the azimuthal magnetic field waveforms.

4.6 Return Stroke

4.6.5 – Properties of the return-stroke channel

- Physical properties of the lightning channel, that can be estimated from the time-resolved optical spectra of return strokes:

- Typical peak temperatures, determined from the ratios of the intensities of spectral lines, were of the order of 28000–31000 K.
- Electron densities in lightning return strokes were determined from a comparison of the measured Stark width of the H_{α} line radiated by hydrogen atoms with theory
 - From Orville (1968), the electron density was $8 \times 10^{17} \text{ cm}^{-3}$ in the first 5 μs , decreasing to $(1-1.5) \times 10^{17} \text{ cm}^{-3}$ at 25 μs , and remaining approximately constant at 50 μs .

Table 4.9. *Estimated characteristics of the lightning channels associated with various processes of the lightning discharge. Adapted from Rakov (1998)*

Channel characteristics ^a	Pre-dart-leader channel (ahead of dart-leader front)	Pre-return-stroke channel (behind dart-leader front and ahead of return-stroke front)	Return-stroke channel (behind return-stroke front)
Temperature, K	~ 3000	$\geq 20\,000$	$\geq 30\,000$
Conductivity, S m^{-1}	~ 0.02	~ 10^4	~ 10^4
Radius, cm	~ 3	~ 0.3	~ 3
R , $\Omega \text{ m}^{-1}$	~ 18 000	~ 3.5	~ 0.035

^a For comparison, the electrical conductivity of carbon is $3 \times 10^4 \text{ S m}^{-1}$, of seawater is 4 S m^{-1} , and of copper is $5.8 \times 10^7 \text{ S m}^{-1}$ (Sadiku 1994); the temperature of the solar interior is 10^7 K and of the solar surface is 6000 K, and the temperatures at which tungsten and lead melt are 3600 K and 600 K, respectively (Halliday and Resnick 1974).

- RAKOV, V. A., & UMAN, M. A. (2003). *Lightning: physics and effects*. Cambridge, U.K., Cambridge University Press;
- **SI¹**: Modelling of the negative discharge in long air gaps under impulse voltages, J H Rakotonandrasana *et al* 2008 *J. Phys. D: Appl. Phys.* 41 105210;
- **SI²**: Biagi, C. J., M. A. Uman, J. D. Hill, D. M. Jordan, V. A. Rakov, and J. Dwyer (2010), Observations of stepping mechanisms in a rocket-and-wire triggered lightning flash, *J. Geophys. Res.*, 115, D23215, doi:10.1029/2010JD014616;
- **SI³**: Arcanjo et al.: *On the interpeak interval of unipolar pulses of current preceding the return stroke in negative CG lightning*. EPSR <https://doi.org/10.1016/j.epsr.2019.03.028>.